Mode-Locked Two-Photon States

Y. J. Lu, R. L. Campbell, and Z. Y. Ou

Department of Physics, Indiana University–Purdue University Indianapolis, 402 North Blackford Street, Indianapolis, Indiana 46202, USA

(Received 23 May 2003; published 17 October 2003)

The concept of mode locking in laser is applied to a two-photon state with frequency entanglement. Cavity enhanced parametric down conversion is found to produce exactly such a state. The mode-locked two-photon state exhibits a comblike correlation function. An unbalanced Hong-Ou-Mandel type interferometer is used to measure the correlation function. A revival of the typical interference dip is observed. We will discuss a scheme for engineering of quantum states in time domain.

DOI: 10.1103/PhysRevLett.91.163602 PACS numbers: 42.50.Dv, 03.65.Ud, 42.50.Ar, 42.65.Ky

Parametric down-conversion process is known to produce two-photon state with entanglement in a variety of degrees of freedom such as polarization [1], phases [2], frequency [3], and angular momentum [4]. Because of its relative ease of production, polarization entanglement is mostly used in applications in quantum information [5,6]. More recently, attention has been focused on the transverse spatial entanglement [7]. With new degrees of entanglement discovered, there are more possibilities for information encoding. Among the entanglement properties, seldom discussed is the temporal entanglement. This is not a surprise if we learn the fact that the bandwidth ($\sim 10^9$ Hz) of current photodetectors cannot match that of the down conversion ($\sim 10^{12}$ Hz). Nevertheless, frequency (complementary to time) entanglement was investigated recently for the potential nonlocal temporal shaping [8]. A similar investigation was done earlier by Zou *et al.* [9]. Entanglement in the frequency and time domain involves infinite dimensions of continuous Hilbert space and therefore should exhibit far richer physical phenomena. In this Letter, we will study directly the temporal entanglement in a special situation similar to a mode-locked laser and propose a scheme for quantum state engineering in the time domain by two-photon interference.

The process of type-I parametric down conversion (PDC) pumped by a field of frequency ω_p produces a two-photon state of a simple spectral structure [10]:

$$|\Phi\rangle_{\mathrm{PDC}} = \int d\Omega\, \phi(\Omega) e^{i(\omega_p/2-\Omega)\delta t} \times \hat{b}^\dagger(\omega_p/2+\Omega)\hat{b}^\dagger(\omega_p/2-\Omega)|\mathrm{vac}\rangle, \quad (1)$$

where $\phi(\Omega)$ gives a continuous spectrum of down conversion and δt sets a relative delay between the two photons. As seen in Eq. (1), the two photons are correlated in frequency. Furthermore, the two photons are also correlated in time with a two-photon correlation function:

$$\Gamma^{(2)}_{\mathrm{PDC}}(\tau) \equiv \langle \hat{E}^{(-)}(t)\hat{E}^{(-)}(t+\tau)\hat{E}^{(+)}(t+\tau)\hat{E}^{(+)}(t)\rangle = |f(\tau-\delta t)|^2, \quad (2)$$

with

$$\hat{E}^{(+)}(t) = \int d\omega \hat{b}(\omega) e^{-i\omega t} \quad \text{and}$$

$$f(\tau) = \int d\Omega\, \phi(\Omega) e^{-i\Omega\tau}.$$

$\Gamma^{(2)}_{\mathrm{PDC}}(\tau)$ is a singly peaked function centered at δt. Normally, the bandwidth of PDC is of the order of 10^{12} Hz producing an extremely short correlation time of subpicosecond. Narrow band two-photon state was recently generated with a correlation time of 10 ns [11].

The concept of mode locking was first introduced to produce short pulses from a laser [12]. Normally, a free running laser emits optical fields in continuous waves (CW) which may consist of many independent longitudinal modes of different frequencies. When the modes of the laser are locked in phase, the output field becomes pulsed in a quasi-CW manner. The emitted pulses are spaced by the cavity round trip time of the laser. The temporal behavior of the field is simply a reflection of the Fourier transformation of the phase-locked frequency spectrum. For two-photon state, we can apply a similar concept. Instead of the continuous spectrum in Eq. (1), we consider discrete modes of equal spacing. The result is a mode-locked two-photon state of the form

$$|\Psi\rangle_{ML} = \sum_{m=-N}^{N} \int d\Omega\, \psi(\Omega + m\Delta\Omega) \times \hat{a}^\dagger(\omega_p/2+\Omega)\hat{a}^\dagger(\omega_p/2-\Omega)|\mathrm{vac}\rangle, \quad (3)$$

where N is the number of frequency modes of correlated photons, $\Delta\Omega$ is the frequency spacing between the adjacent modes, and $\psi(\Omega)$ gives the spectral distribution for a single mode. Different modes of photon pairs are in superposition, which provides the mechanism for phase locking. Such a state can be generated from a wide band parametric down conversion [given in Eq. (1)] filtered by a Fabry-Perot cavity (Fig. 1). The different frequency components come from the longitudinal modes of the cavity. $\Delta\Omega$ is then the free spectral range of the cavity. All the pairs have a common origin (phase) from the pump field. Similar to Eq. (2), the two-photon time

correlation function can be easily calculated for this state:

$$\Gamma^{(2)}_{ML}(\tau) = |g(\tau)F(\tau)|^2, \tag{4}$$

where

$$g(\tau) = \int d\Omega \psi(\Omega) e^{-i\Omega\tau}, \qquad F(\tau) = \frac{\sin[(2N+1)\Delta\Omega\tau/2]}{\sin(\Delta\Omega\tau/2)}.$$

Since $\psi(\Omega)$ is the spectrum of single mode, it has much narrower bandwidth than the full bandwith $N\Delta\Omega$. So $g(\tau)$ is a slowly varying function and $\Gamma^{(2)}(\tau)$ is mainly determined by the function $F(\tau)$, which has a comblike shape (Fig. 1). The period of $F(\tau)$ is the cavity round trip time $t_r = 1/\Delta\Omega$. The physics behind Eq. (4) is the following: when a pair of photons enter the filter cavity, the cavity makes them bounce back and forth. Only when they hit the output coupler, is there some finite probability of escape and being detected. So the coincidence occurs only at a time interval that is a multiple of the round trip time of the cavity.

The comblike time correlation function in Eq. (4) should be directly observable in a time delay distribution measurement, provided that the resolution time T_R of the detectors is smaller than the time interval $t_r = 1/\Delta\Omega$. Otherwise, the result is an average over the resolution time T_R in many periods of t_r:

$$\Gamma^{(2)}_{\text{av}}(\tau) = A|g(\tau)|^2, \tag{5}$$

where A is a constant. So in the case of a poor detector resolution time, only the general contour of $\Gamma^{(2)}(\tau)$ can be observed and the comblike feature is lost.

However, the comblike feature in Eq. (4) can be indirectly observed by the method of two-photon interference with a variation of Hong-Ou-Mandel (HOM) interferometer [13] as shown in Fig. 2. For a collinear type-I parametric down conversion, the two correlated photons copropagate and can be separated by a beam splitter (BS1). The second beam splitter (BS2) recombines the two photons to form the HOM interferometer. The whole setup is just a Mach-Zehnder interferometer. With two-photon detection at the outputs, it is also a Franson-type interferometer when the paths of the two arms are not balanced [14,15]. In a simple single mode model, the first beam splitter (BS1) transforms the input two-photon state into the following state:

$$|\Psi\rangle_{BS1} = (|2,0\rangle + |0,2\rangle + \sqrt{2}|1,1\rangle)/2. \tag{6}$$

The first two terms give the usual Franson-type two-photon interference (between short-short and long-long paths) while the last term has no interference effect when the path difference is larger than the coherence length and normally provides a constant background if the detectors cannot resolve between the short and long paths. This limits the maximum visibility to 50% [15]. With mode-locked two-photon input, however, the comblike correlation function indicates that the $|1,1\rangle$ state will reappear at a path delay of every multiple of ct_r, the round trip distance of the filter cavity. When this happens, the last term will exhibit Hong-Ou-Mandel interference dip [13] at nonzero delays. The revival of HOM interference dips was first predicted by Shapiro [16].

The intuitive argument above can be easily confirmed by a calculation of the two-photon coincidence rate between the two detectors at the output of the unbalanced Mach-Zehnder interferometer in Fig. 2. We use a multimode state given in Eq. (3) as the input state to the interferometer. We first calculate the correlation function

$$\Gamma^{(2)}_{12}(\tau) = \langle \hat{E}^{(-)}_1(t)\hat{E}^{(-)}_2(t+\tau)\hat{E}^{(+)}_2(t+\tau)\hat{E}^{(+)}_1(t)\rangle$$

and then integrate over the coincidence window T_R of the detectors. The result is the two-photon coincidence rate and is given with 50:50 beam splitters as follows:

$$R_2(\Delta T) = \int_{T_R} d\tau \Gamma^{(2)}_{12}(\tau) \propto (1 - \cos\omega_p \Delta T) + (1 - V), \tag{7}$$

where

$$V = \frac{\int_{T_R} d\tau F(\tau + \Delta T) g(\tau + \Delta T) F(\tau - \Delta T) g(\tau - \Delta T)}{\int_{T_R} d\tau |g(\tau)F(\tau)|^2}.$$

The first term in Eq. (7) corresponds to the first two terms in Eq. (6) and produces a phase sensitive two-photon interference pattern. The second term in Eq. (7) arises from the last term in Eq. (6) and gives rise to the HOM interference dip as ΔT is scanned. Normally, there is only one dip around zero delay ($\Delta T \approx 0$). But for mode-locked two-photon state, the reappearance of the coincidence peak at nonzero delays (due to the comblike correlation

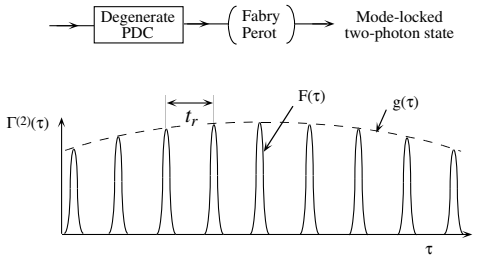

FIG. 1. Simple scheme for the generation of a mode-locked two-photon state and its comblike time correlation function.

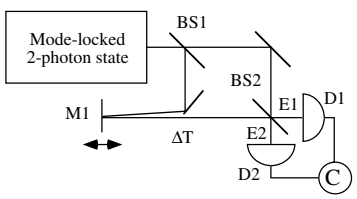

FIG. 2. Layout of the interferometer. ΔT is the time delay between the two arms.

function) will revive the HOM dips every time when the time delay ΔT is such that $F(\tau + \Delta T)$ overlaps with $F(\tau - \Delta T)$ to produce $V = 1$. This corresponds to $\Delta T = Mt_r/2$ with $M =$ integer. A surprising result is that the period of the revival of HOM dip is $t_r/2$ rather than t_r predicted from a previous simple intuitive argument and Ref. [16]. The shorter period can be understood if we take a detailed look at the timeline of photodetection in Fig. 3 of an unbalanced HOM interferometer. The figure shows the interference of two possibilities: both photons are transmitted or reflected. In each case, $2(l_1 - l_2)$ is the path difference between the two arms of the interferometer. Figure 3(a) corresponds to the intuitive argument: the two photons come from adjacent coincidence peaks with $\Delta T = t_r$. In Fig. 3(b), photodetections of the two photons are not simultaneous but have a time difference of $t_c/2$ [17]. The two overlapping possibilities are from two different cases: two photons are separated by a delay of t_r or they are simultaneous. Because of mode lock nature of the process, the two possibilities are coherent to each other and will produce interference. In this case, we only need a time delay ΔT to be $t_r/2$.

Although filtering after the generation of parametric down-converted photons will produce the required mode-locked two-photon state, it is at the expense of signal level because the down-converted light signal is proportional to the detection bandwidth. Recently we have successfully implemented a scheme of cavity enhanced parametric down conversion for the generation of narrow band two-photon state without the reduction of the signal level [11]. In this scheme, a temperature stablized $KNbO_3$ crystal is placed inside a cavity and is pumped by a frequency doubled Ti-sapphire laser. The laser is operated at 855 nm. The detail of the system is described in Ref. [11]. Multimode operation of the device produces naturally a mode-locked two-photon state. The cavity round trip time of the device is of the order of 40 ps, which prevents us from direct observation of the comb-like correlation function in Eq. (4). Nevertheless, we did observe the time average behavior predicted in Eq. (5) in a time delay distribution measurement.

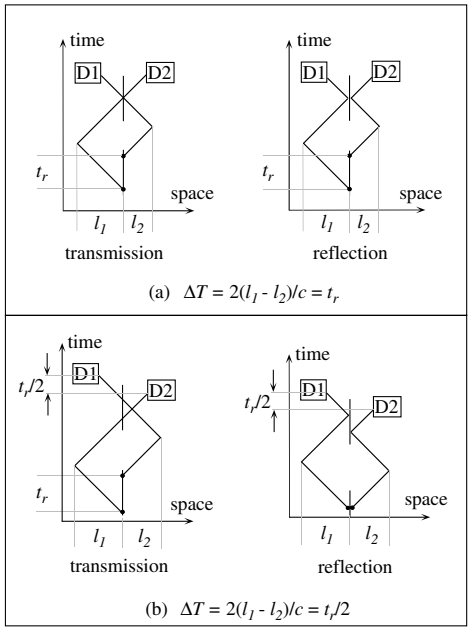

FIG. 3. Timeline for photodetection of two photons in an unbalanced HOM interferometer. See text for details.

To indirectly show the mode locking effect, we input the state into an unbalanced Mach-Zehnder interferometer as sketched in Fig. 2 and observe the coincidence count between the two outputs as the mirror M1 is scanned. The mirror M1 is mounted on a piezoelectric transducer for phase scan and a micrometer for large range location scan. The coincidence window is measured to be 10 ns. Under this condition ($T_R = 10$ ns $\gg \Delta T \sim$ 10 ps). The coincidence rate is given by Eq. (7). The first term of Eq. (7) is a phase dependent term that is always there. In order to concentrate on the second term in Eq. (7) for unbalanced HOM interference effect, we dither the phase (piezoelectric transducer) so that the contribution from the first term is merely a constant baseline that will limit the HOM interference visibility to a maximum of 50%. In Fig. 4, we plot the corrected coincidence counts as a function of the position of M1 (μm). The reappearance of the HOM dip at nonzero delays in Fig. 4 implies a two-photon correlation function as in Eq. (4) [16]. The data were collected in separate runs because the interferometer needs to be realigned after some large displacement of M1 (the visibility of the interferometer, which is independently monitored by an auxiliary laser, drops significantly after about 6 mm displacement of M1). So the coincidence data has to be normalized to an average of the points at the wings of the dips. The spacing between dips is 5.75 mm corresponding to one half cavity round trip distance of the cavity as predicted in Eq. (7).

Next we fix the micrometer position of M1 at the bottoms of the two dips in Fig. 4, which correspond to path differences of one half and one full cavity round trip

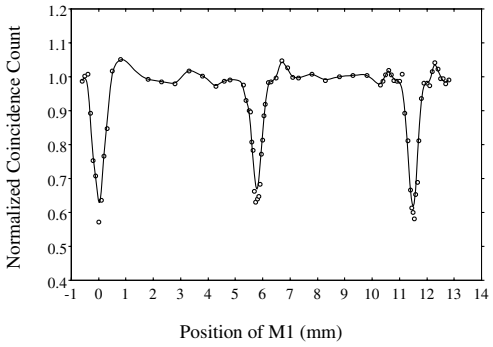

FIG. 4. Normalized coincidence as a function of the micrometer position of mirror M1. The solid line is a smooth interpolation of the data for visual guidance.

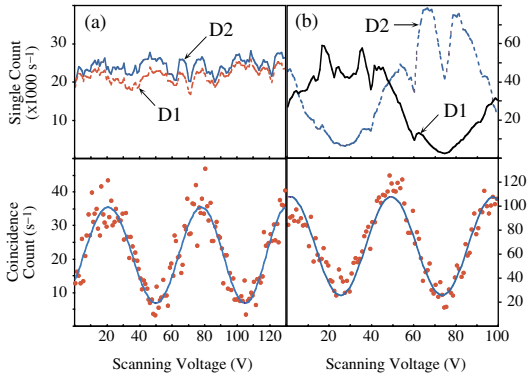

FIG. 5 (color online). Coincidence as well as single counts as a function of the voltage of piezoelectric transducer. Micrometer for M1 is set at (a) 5.7 mm and (b) 11.5 mm (see Fig. 4 for reference).

distance, respectively. We then scan the phase via the piezoelectric transducer. Each run takes about 2 min. Figure 5 shows the coincidence as well as the single detector counts as a function of electric voltage at those 2 μm positions of M1. Coincidence counts in both runs show interference pattern with visibility larger than 50%. The solid curves are a least square fit to a SINE function with 68% and 62% visibility, respectively. The low visibility is attributed to poor mode match at large path delays. Work is underway to replace the beam splitters with fiber couplers to improve the mode match and also avoid the realignment problem in the experiment leading to Fig. 4. Surprisingly, Fig. 5(b) shows interference in the single detector counts at nonzero delay that is larger than coherence length and the counts from the two detectors are 180° out of phase (the unexpected drops in single counts are due to instability of the cavity during data taking and are corrected in coincidence counts). So the interference pattern in coincidence in Fig. 5(b) is simply from the anticorrelation of single counts. This is not fourth-order but second-order interference. Only Fig. 5(a) shows genuine fourth-order interference and is a result of the quantum entanglement in Eq. (3). The single count behavior in Fig. 5 can be understood from the second-order field correlation function for the state in Eq. (3):

$$\gamma(\tau) = \langle \hat{E}^{(-)}(t+\tau)\hat{E}^{(+)}(t)\rangle = e^{i\omega_p\tau/2}G(\tau)F(\tau), \qquad (8)$$

with $G(\tau) = \int d\omega |\psi(\omega)|^2 e^{i\omega\tau}$. $|\gamma(\Delta T)|$ gives the visibility of interference patterns in single detector counts and it has a similar comblike shape as $\Gamma^{(2)}_{ML}(\tau)$ in Eq. (4). So the single count interference pattern revives at various multiples of t_r, just like a mode-locked laser. In contrast, interference pattern in coincidence occurs with a period of $t_r/2$. For those M1 positions that are not inside any of the dips in Fig. 4, we observed a visibility of around 35% in coincidence. This corresponds to the Franson interferometer of maximum visibility of 50% [14,15].

The interesting comblike correlation function can be used for quantum state engineering. Here we propose to use two-photon interference to take out any spike in the correlation function (Fig. 1). To do that, we mix a wide band two-photon state described in Eqs. (1) and (2) with a mode-locked two-photon state in Eq. (3), say, by a beam splitter. For the resultant field, we find that

$$\Gamma^{(2)}(\tau) \propto |g(\tau)F(\tau) - f(\tau - \delta t)|^2. \qquad (9)$$

If $f(\tau - \delta t)$ overlaps with one of the peaks of $F(\tau)$, complete destructive interference will take out that peak in $\Gamma^{(2)}(\tau)$ with a proper adjustment of relative strength of the two incoming fields. By changing the delay δt, we can manage to take any one out for information coding.

We would like to thank P. Kumar for pointing us to Ref. [16] and suggesting a possible experiment. This work was supported by Purdue Research Foundation and NSF.

[1] Y. H. Shih and C. O. Alley, Phys. Rev. Lett. **61**, 2921 (1988); Z. Y. Ou and L. Mandel, *ibid.* **61**, 50 (1988).
[2] P. Grangier, M. J. Potasek, and B. Yurke, Phys. Rev. A**38**, 3132 (1988).
[3] Z. Y. Ou and L. Mandel, Phys. Rev. Lett. **61**, 54 (1988).
[4] H. H. Arnaut and G. A. Barbosa, Phys. Rev. Lett. **85**, 286 (2000); A. Mair, A. Vaziri, G. Weihs, and A. Zeilinger, Nature (London) **412**, 313 (2001).
[5] K. Mattle, H. Weinfurter, P. G. Kwiat, and A. Zeilinger, Phys. Rev. Lett. **76**, 4656 (1996).
[6] D. Bouwmeester, J.-W. Pan, K. Mattle, M. Eibl, H. Weinfurter, and A. Zeilinger, Nature (London) **390**, 575 (1997).
[7] S. P. Walborn, A. N. de Oliveira, S. Padua, and C. H. Monken, Phys. Rev. Lett. **90**, 143601 (2003).
[8] M. Bellini, F. Marin, S. Viciani, A. Zavatta, and F. T. Arecchi, Phys. Rev. Lett. **90**, 043602 (2003).
[9] X. Y. Zou, T. P. Grayson, and L. Mandel, Phys. Rev. Lett. **69**, 3041 (1992).
[10] R. Ghosh, C. K. Hong, Z. Y. Ou, and L. Mandel, Phys. Rev. A**34**, 3962 (1986).
[11] Z. Y. Ou and Y. J. Lu, Phys. Rev. Lett. **83**, 2556 (1999); Y. J. Lu and Z. Y. Ou, Phys. Rev. A**62**, 033804 (2000).
[12] See, for example, A. E. Siegman, *Lasers* (University Science Books, Mill Valley, California, 1986).
[13] C. K. Hong, Z. Y. Ou, and L. Mandel, Phys. Rev. Lett. **59**, 2044 (1987).
[14] J. D. Franson, Phys. Rev. Lett. **62**, 2205 (1989).
[15] Z. Y. Ou, X. Y. Zou, L. J. Wang, and L. Mandel, Phys. Rev. Lett. **65**, 321 (1990); P. G. Kwiat, W. A. Vareka, C. K. Hong, H. Nathel, and R. Y. Chiao, Phys. Rev. A**41**, 2910 (1990).
[16] J. H. Shapiro, in *Technical Digest of Topical Conference on Nonlinear Optics* (Optical Society of America, Washington, DC, 2002), p. 440, FC7-1.
[17] T. B. Pittman *et al.*, Phys. Rev. Lett. **77**, 1917 (1996).